

**Electronic Supplementary Information**

31 October, 2012

Ms. ID: LC-ART-08-2012-040993

**Electrochemical Detection of Individual DNA Hybridization Events**

Timothy M. Alligrant, Elizabeth G. Nettleton, Richard M. Crooks

(12 Pages)

**Table of Contents**

Characterization of Platinum Nanoparticles and Preparation of Platinum Nanoparticle-DNA Conjugates	S3
Device Fabrication Details	S4
Additional Electrochemical Data	S4
Additional Experimental Details	S10
Device Characterization	S11
References	S12

## Characterization of Platinum Nanoparticles and Preparation of PtNP-DNA Conjugates

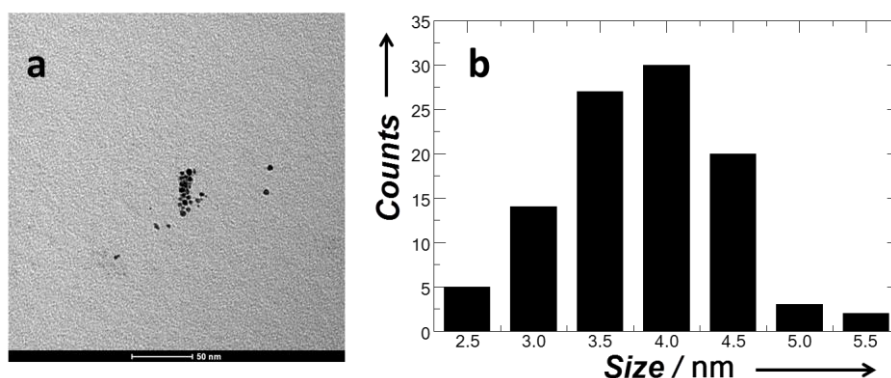


**Fig. S1.** (a) TEM image of the PtNP tags used in this study. (b) The corresponding size-distribution histogram.

To characterize the prepared PtNPs by TEM, 1.0  $\mu\text{L}$  of the dialyzed PtNP solution was diluted in 500.0  $\mu\text{L}$  of deionized water. Then, in an attempt to disperse the NPs for imaging, the pH of this solution was increased to  $\sim 7$  using 0.1 M NaOH. This ensures that the citrate capping agent on the PtNPs is negatively charged. Next, a 2.0  $\mu\text{L}$  aliquot of this diluted PtNP solution was placed on a carbon-coated Cu grid (EM Sciences, Gibbstown, NJ) followed by solvent evaporation in air. Fig. S1 presents a representative TEM image of the PtNPs and a size-distribution histogram generated using several such micrographs. The size-distribution histogram was generated by measuring 100 individual PtNPs utilizing Gatan Digital Micrograph software (v 3.11.2, Gatan, Inc., Pleasanton, CA), and the average particle size was found to be  $4.0 \pm 0.7$  nm.

To prepare the PtNP-cDNA conjugates, it was necessary to know the concentration of the PtNP stock solution. The PtNP concentration was determined in a manner similar to that reported by Bard and coworkers.<sup>1</sup> Specifically, the nanoparticle

concentration is equal to the concentration of the Pt precursor divided by the average number of Pt atoms contained in an average-sized particle. From knowledge of the average PtNP size (Fig. S1) and the work of Jentys, each PtNP is expected to contain ~1800 Pt atoms.<sup>2</sup> Therefore, the PtNP concentration in the stock solution is ~1800 times smaller than that of the Pt precursor, or 500 nM. So, the PtNP-cDNA conjugates were prepared by mixing a 25:1 molar ratio of cDNA:PtNPs and allowing them to react at 24-25 °C for no less than 2 h prior to use.

### Device Fabrication Details

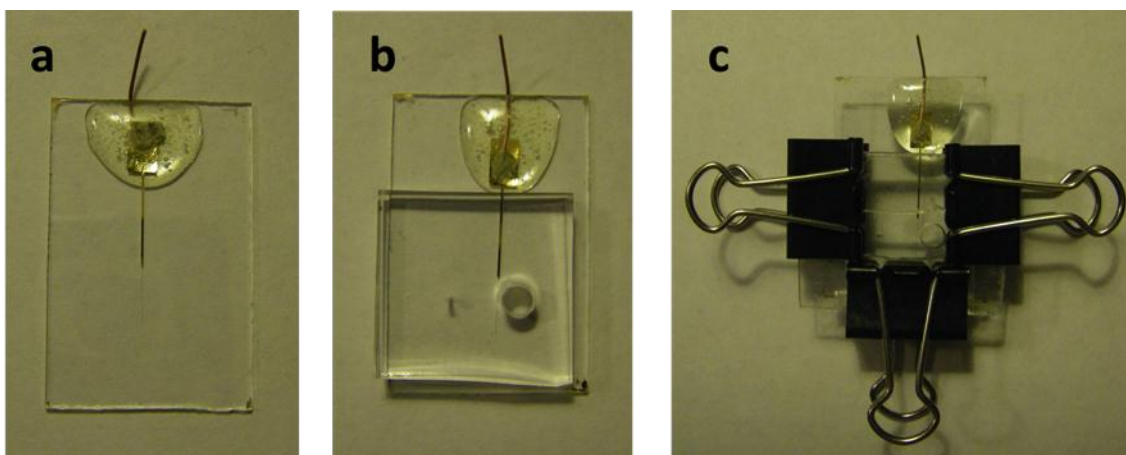


**Fig. S2.** Fabrication of the microelectrochemical device. (a) Au on glass slide after Au etching, acetone wash, and connection of the copper lead. (b) After bonding of the PDMS monolith. (c) The fully assembled device.

### Additional Electrochemical Data

The electrochemistry of  $N_2H_4$  was evaluated using microelectrochemical devices having Pt and Au working electrodes, as well as using standard UMEs. The data in Fig. S3a were obtained in microelectrochemical devices, and the CVs here compare the oxidation of 0 and 5.0 mM  $N_2H_4$  solutions at a 20  $\mu\text{m}$  x 25  $\mu\text{m}$  Pt electrode to the oxidation of 15.0 mM  $N_2H_4$  at a 25

$\mu\text{m} \times 25 \mu\text{m}$  Au electrode under flow ( $50 \text{ nL min}^{-1}$ ). The CV measured on Pt in the absence of  $\text{N}_2\text{H}_4$  is included to assess the effect of  $\text{O}_2$  reduction on the electrochemical measurements. This is important because the solutions in the microfluidic cells were not deaerated. Comparison of the CVs obtained at the Pt

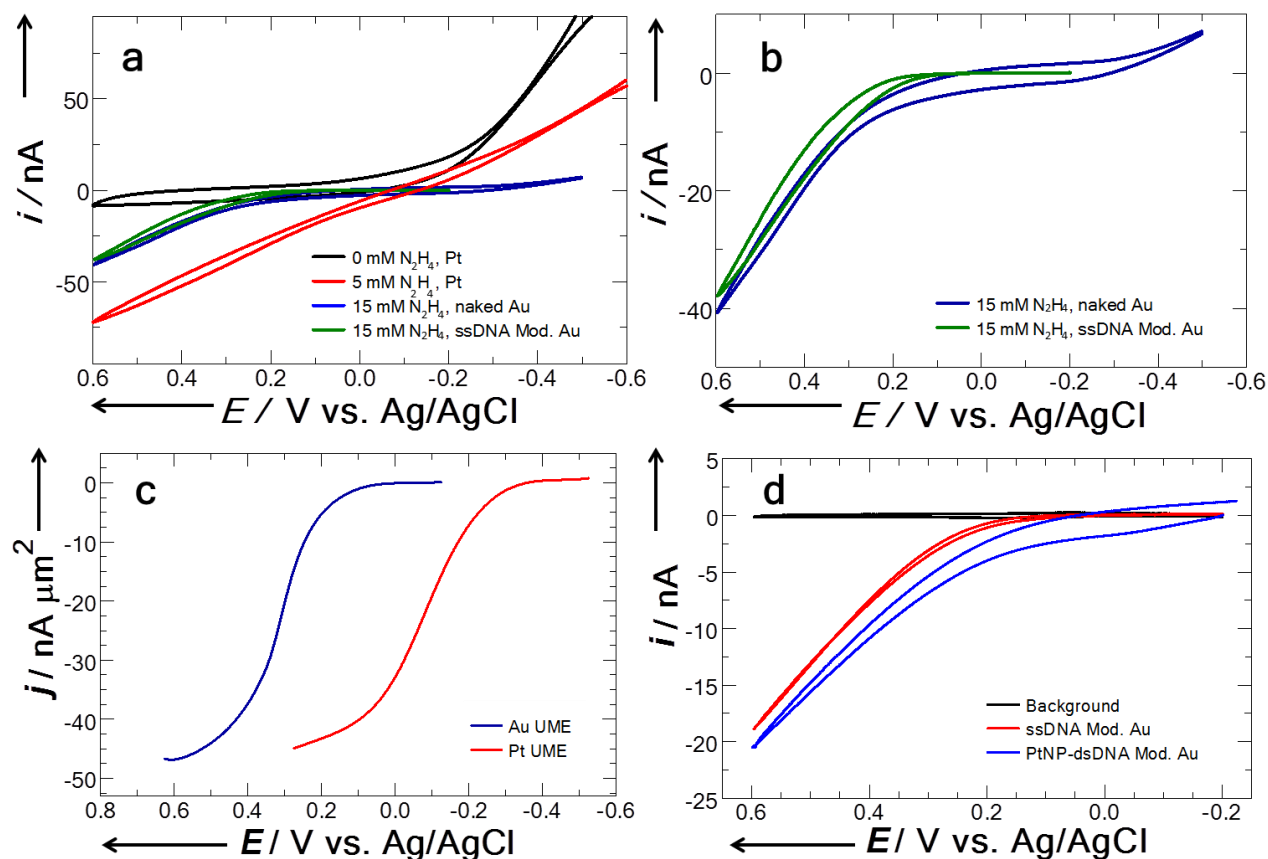


**Fig. S3.** CVs obtained at modified and naked Au and Pt electrodes. The electrode material and modifications are provided in the legends. The Pt and Au electrodes in the microelectrochemical devices were  $20 \mu\text{m} \times 25 \mu\text{m}$  (Frame a) and  $25 \mu\text{m} \times 25 \mu\text{m}$  (Frames a, b and d), respectively. The CVs in (b) are expanded versions of the corresponding CVs in (a). The ultramicroelectrodes (UMEs, Frame c) had radii of  $12.5 \mu\text{m}$  (Au) and  $10 \mu\text{m}$  (Pt), respectively, and current is given as current density ( $j$ ). The electrolyte was  $50.0 \text{ mM}$  phosphate buffer, pH 7.0. The concentration of  $\text{N}_2\text{H}_4$  was  $5.0 \text{ mM}$  in frames (c) and (d). Scan rate =  $20 \text{ mV s}^{-1}$  and potentials are vs. Ag/AgCl. Only the solution used to obtain the data in Frame c was deaerated.

electrodes indicates that the onset potential for  $\text{N}_2\text{H}_4$  oxidation is at  $\sim 0$  V. However, the onset potential for  $\text{N}_2\text{H}_4$  oxidation on bare and ssDNA-modified Au is at  $\sim 0.2$  V vs. Ag/AgCl, as shown in Fig. S3b, which is an expanded version of the relevant potential region in Fig. S3a.

To facilitate the comparison of  $\text{N}_2\text{H}_4$  oxidation on Au and Pt electrodes, experiments were also performed on naked UMEs in deaerated solutions (Fig. S3c). Similar to the Au microelectrochemical devices, the onset of  $\text{N}_2\text{H}_4$  oxidation on Au is  $\sim 0.2$  V, while the onset potential on the Pt UME is  $\sim -0.2$  V.

Fig. S3d compares CVs obtained using microelectrochemical devices having Au electrodes modified with ssDNA and PtNP-dsDNA. The important result is that the oxidation potential for  $\text{N}_2\text{H}_4$  shifts negative in the presence of the PtNP label. The PtNP-dsDNA modification was carried out as follows. The electrode was washed in acetone, dried with a stream of  $\text{N}_2$ , then a  $30.0 \mu\text{L}$  drop of  $1.0 \mu\text{M}$  ssDNA solution in TE buffer was placed on the electrode for 2 h, the electrode was washed with DI  $\text{H}_2\text{O}$  for 20 s, and dried with a stream of  $\text{N}_2$ . The surface coverage of DNA was quantified using the procedure described in the main text, and then a  $60.0 \mu\text{L}$  aliquot of  $100 \text{ nM}$  PtNP-cDNA in  $0.1 \text{ M}$  phosphate buffer (pH 7.0) was placed on the electrode surface for 2 h in a humidity chamber ( $20\text{--}25 \text{ }^\circ\text{C}$ ,  $85\text{--}90 \%$  humidity). Next, the device was washed with  $0.1 \text{ M}$  phosphate, pH 7.0 for 20 s, dried with  $\text{N}_2$  and then the hybridization efficiency was determined. Hybridization efficiency is defined as the percentage of cDNA bound to ssDNA. The electrode used to obtain the data in Fig. S3d had a hybridization efficiency of  $\sim 9\%$ . Next, an air plasma cleaned PDMS monolith was mechanically clamped to the glass slide and the CV in Fig. S3d was measured as previously described. In addition to this, confirmation of DNA

hybridization by PtNP-labeled DNA, Fig. S6 also provides XPS results of DNA modified Au/glass substrates.

Two control experiments were performed to determine the degree to which nonspecific adsorption (NSA) contributes to the observed current transients. The first experiment involved flowing PtNP-cDNA over naked Au electrodes, while the second involved flowing naked PtNPs over ssDNA-modified Au electrodes. Fig. S4 presents representative  $i-t$  data for these control experiments in a solution containing 15.0 mM  $N_2H_4$ . The black and blue  $i-t$  curves in Fig. S4 were measured while flowing 0 and 50 pM PtNP-cDNA, respectively, over a naked Au electrode. While the green and brown  $i-t$  curves were measured while flowing 0 and 50 pM naked PtNPs, respectively, over a ssDNA-modified Au electrode. For both control experiments in Fig. S4 no current transients were observed, indicating that NSA does not contribute to the observation of current transients under these conditions. An  $i-t$  curve exhibiting current transients (red curve) upon flowing PtNP-cDNA over the ssDNA-modified Au

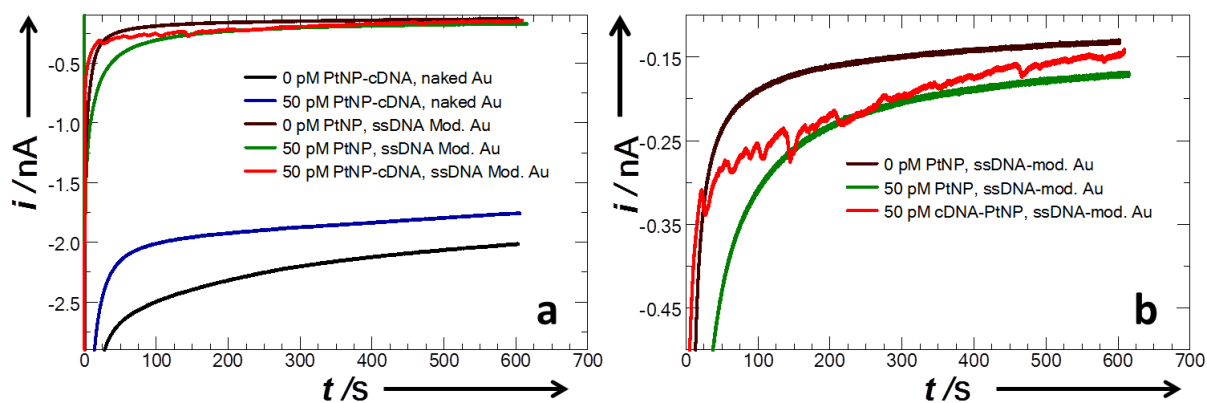


**Fig. S4.** The  $i-t$  results for control experiments obtained in solutions containing 15.0 mM  $N_2H_4$  and 50.0 mM phosphate buffer, pH 7.0. At  $t = 0$ , the electrode potential was stepped from  $-0.2$  V to  $0.15$  V. The electrode size was  $25 \mu m \times 25 \mu m$ , and the solution flow rate was  $50 \text{ nL min}^{-1}$ . Other experimental conditions are provided in the legends. Frame (b) is an expanded view of the results in (a).

electrode in 15.0 mM  $\text{N}_2\text{H}_4$  is also presented for comparison. The current transients observed in the red  $i$ - $t$  curve exhibited an average peak current of  $24 \pm 10$  pA. Fig. S4b is an expanded view of Fig. S4a showing a smaller current range.

To evaluate the current transient data used to construct Fig. 3 in the main text, one  $i$ - $t$  curve at each  $\text{N}_2\text{H}_4$  concentration (5 to 20 mM) is displayed in Fig. S5. An inset is included in each representative  $i$ - $t$  curve to show the scale of the observed current transients. The average peak currents were: (a)  $29 \pm 16$  pA, 5 mM  $\text{N}_2\text{H}_4$ ; (b)  $38 \pm 23$  pA, 7.5 mM  $\text{N}_2\text{H}_4$  (c)  $67 \pm 30$  pA, 10 mM  $\text{N}_2\text{H}_4$ ; (d)  $24 \pm 10$  pA, 15 mM  $\text{N}_2\text{H}_4$ ; and (e)  $17 \pm 8$  pA, 20 mM  $\text{N}_2\text{H}_4$ . These experimentally determined values can be compared to values calculated using eq 2 in the text: 31 pA at 5 mM; 46 pA at 7.5 mM; 61 pA at 10 mM; 92 pA at 15 mM; and 104 pA at 20 mM. Fig. 3 from the main text is reproduced in Fig. S5f as a reference.



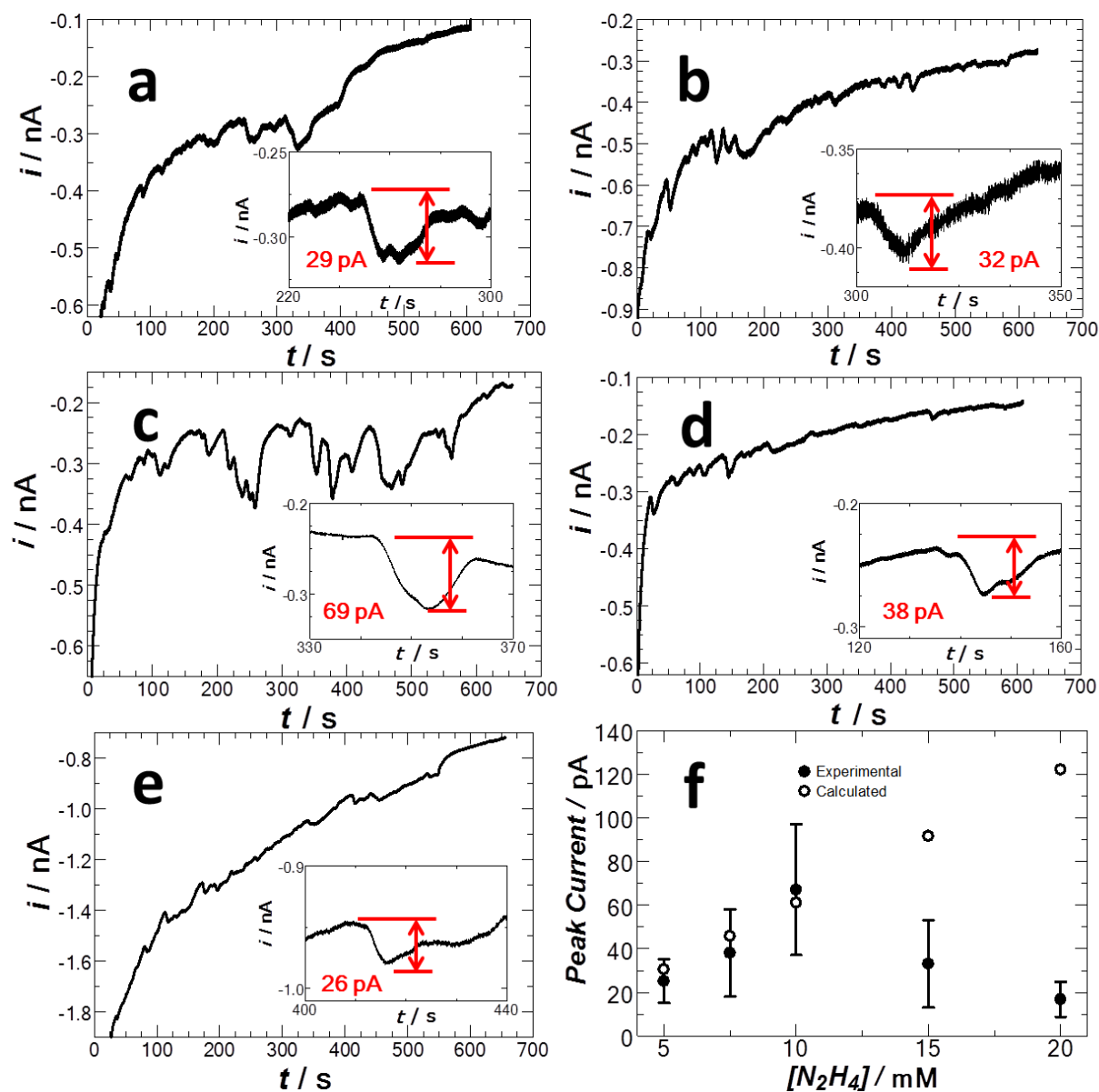


**Fig. S5.** Representative  $i$ - $t$  curves at (a) 5; (b) 7.5; (c) 10; (d) 15; and (e) 20 mM  $N_2H_4$ . The insets represent an expanded region of each  $i$ - $t$  curve. For each plot, the PtNP-cDNA conjugate concentration was 25 pM in 50 mM phosphate buffer, pH 7, and the flow rate was 50 nL min<sup>-1</sup>. (f) A plot of the average magnitude of the current transients arising from electrocatalytic  $N_2H_4$  oxidation as a function of the concentration of  $N_2H_4$  (same as Fig. 3 in the main text).

#### Additional Experimental Details

Due to the low (50.0 mM) buffer concentration used in these experiments, the addition of concentrated  $N_2H_4$  increased the pH of the solutions. Therefore, prior to use, the pH of the  $N_2H_4$  solutions was adjusted to pH 7.0 using 0.5 M HCl.

Prior to each microelectrochemical measurement described in the text, the following sequence of events occurred. (1) The tubing bearing the  $N_2H_4$  solution was inserted into a reservoir in the PDMS monolith. (2) 40.0  $\mu$ L of buffer (black CV in Fig. 2a) or  $N_2H_4$  + buffer (red CV in Fig. 2a, and black, green and red traces in Fig. 2b) solution were placed in the fluidic outlet to provide an electrical connection for the reference electrode. (3) 15 min was allotted to ensure even flow of solution in the microchannel. This duration was determined on the basis of the time required to ensure reproducible CVs. During this period, -0.20 V was applied to the working electrode to prevent DNA hybridization (when PtNP-DNA conjugates were present). As stated in the text, the applied potential of -0.20 V during flow equilibration was important for three reasons: (1) it is significantly negative of the point-of-zero charge (pzc, 0.2 to 0.3 V), which inhibits hybridization of negatively charged DNA; (2) it is not so negative to significantly affect the conformation of the ssDNA (causing them to stand perpendicular to the Au surface); (3) it is in a potential region where  $N_2H_4$  oxidation does not proceed on a Au electrode. The pzc was determined to be  $\sim$ 0.29 V using AC voltammetry. This value is close to the value of 0.2 V reported by others for similar systems.<sup>3-5</sup>

In addition to the *i-t* measurements obtained at 0.15 V vs. Ag/AgCl described in the text, measurements were also obtained at 0.05 and 0.10 V to determine the lowest potential at which current transients could be observed at ssDNA-modified electrodes. Current transients were not observed when applying

these potentials while flowing 25 to 50 pM PtNP-cDNA. Note that all *i-t* measurements were recorded over ~10 min intervals.

### **Device Characterization**

X-ray photoelectron spectroscopy (XPS) was used to characterize DNA- and PtNP-modified Au substrates. This analysis is important as it provides an additional means of device characterization to demonstrate that ssDNA-modified Au substrates can be labeled with PtNPs. The substrates were prepared similarly to electrodes in the microelectrochemical devices, with the exceptions that they were not photolithographically patterned and they were cleaned somewhat differently prior to modification. Each Au substrate was first rinsed with acetone, dried with N<sub>2</sub>, immersed in piranha solution for 10 min (3:1 mixture of concentrated H<sub>2</sub>SO<sub>4</sub> to 30% H<sub>2</sub>O<sub>2</sub>). Warning: Piranha solution is a strong oxidant and reacts violently with organic materials. It should be handled with care and all work should be performed in a fume hood with the necessary protection gear.). Next, the sample was removed from the piranha solution and thoroughly washed with deionized water. The first substrate was dried with N<sub>2</sub> and set aside for later XPS evaluation. The other two substrates were modified with 60.0 μL of 1.0 μM ssDNA probe in TE buffer for 2 h in a humidity chamber. Next, these samples were each washed with deionized water for 20 s, dried with N<sub>2</sub>, and then one substrate was set aside for XPS analysis. The final substrate was further modified by placing 60.0 μL of 1.0 μM of PtNP-cDNA in hybridization buffer (Sigma) onto its surface, and allowing hybridization to proceed for 2 h in a humidity chamber. The substrate was then washed with pH 7.0, 0.10 M phosphate buffer for 20 s and then dried with N<sub>2</sub>. Next, the substrates were mounted onto the XPS sample holder and

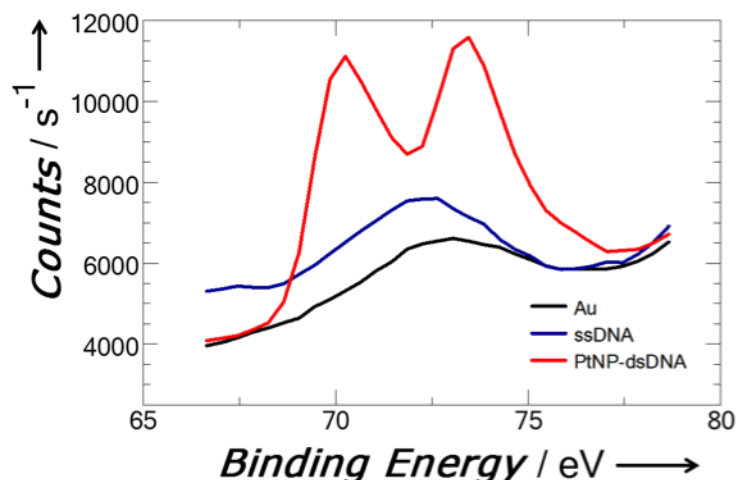


**Fig. S6.** XPS spectra obtained in the Pt 4f region on (black) naked Au; (blue) ssDNA-modified Au, and (red) PtNP-dsDNA-modified Au.

grounded using a strip of copper tape. XPS analyses were performed using a Kratos AXIS Ultra spectrometer (Chestnut Ridge, NY) outfitted with a monochromatic Al K $\alpha$  X-ray source. When charging of the substrate became significant, an electron flood gun was used as a charge neutralizer. High-resolution spectra were collected with a 0.4 eV step size and band pass energy of 80 eV. Fig. S6 shows the spectra obtained from each of the prepared Au samples in the Pt 4f region. Characteristic peak(s) for Pt 4f<sub>7/2</sub> and 4f<sub>5/2</sub> were observed only in the case of the third substrate, which was modified with PtNP labels. The energy axis of each spectra in Fig. S6 was adjusted to the Au 4f<sub>7/2</sub> line at 84.0 eV.<sup>6</sup>

## References

1. X. Xiao, F.-R. F. Fan, J. Zhou and A. J. Bard, *J. Am. Chem. Soc.*, 2008, **130**, 16669-16677.
2. A. Jentys, *Phys. Chem. Chem. Phys.*, 1999, **1**, 4059-4063.
3. U. Rant, K. Arinaga, S. Fujita, N. Yokoyama, G. Abstreiter and M. Tornow, *Nano Lett.*, 2004, **4**, 2441-2445.
4. U. Rant, K. Arinaga, S. Fujita, N. Yokoyama, G. Abstreiter and M. Tornow, *Org. Biomol. Chem.*, 2006, **4**, 3448-3455.
5. E. A. Josephs and T. Ye, *J. Am. Chem. Soc.*, 2012, **134**, 10021-10030.
6. C. D. Wagner, A. V. Naumkin, A. Kraut-Vass, J. W. Allison, C. J. Powell and J. R. Rumble, Jr., *NIST Photoelectron Spectroscopy Database*.